

# Two-cluster bifurcations in systems of globally pulse-coupled oscillators

Leonhard Lücken, Serhiy Yanchuk

November 13, 2018

Institute of Mathematics, Humboldt University of Berlin,  
Unter den Linden 6, 10099 Berlin, Germany

## Abstract

For a system of globally pulse-coupled phase-oscillators, we derive conditions for stability of the completely synchronous state and all possible two-cluster states and explain how the different states are naturally connected via bifurcations. The coupling is modeled using the phase-response-curve (PRC), which measures the sensitivity of each oscillator's phase to perturbations. For large systems with a PRC, which turns to zero at the spiking threshold, we are able to find the parameter regions where multiple stable two-cluster states coexist and illustrate this by an example. In addition, we explain how a locally unstable one-cluster state may form an attractor together with its homoclinic connections. This leads to the phenomenon of intermittent, asymptotic synchronization with abating beats away from the perfect synchrony.

## 1 Introduction

Ensembles of interacting dynamical systems appear as mathematical models in many branches of science [1, 2]. For example, the study of coupled lasers [3, 4, 5, 6] is triggered by technological applications such as high-power generation or secure communication [7, 8]. Interacting biological units play an important role for the functioning of living organisms [9]. Mechanical or electrical coupled oscillators have been extensively studied as paradigmatic models [10, 11] to study various synchronization phenomena. In neuroscience, the synchronization of neuron populations plays an important role [12, 13, 14] and might even lead to pathological effects [15]. As a result, there was recently an increasing effort to control the desynchronization of populations of coupled oscillators. In particular, the coordinated reset stimulation technique [12, 16] proposes to establish a cluster-state in the network, in which the oscillator's phases split into several subgroups. This example illustrates the importance of the analysis of cluster formation in coupled systems.

In this paper we investigate the connection between the properties of single oscillators and their influence on the appearance of clusters in a globally coupled system of such oscillators. We consider the pulse coupling [17, 18, 19, 20, 21] approximation, which is widely used for modeling of neuron populations. Such an approximation is appropriate in the case, when the interaction time between the oscillators is much smaller than the characteristic period of oscillations. The interaction is mediated by the pulses, which are emitted by each of the oscillator after reaching some threshold. Although the coupling topology is fixed and assumed to be global, i.e. all-to-all and homogeneous, the dynamical properties of the individual oscillators will be considered variable (all at the same time). This enables us to describe a bifurcation scenario, which links dynamic regimes of stable synchrony with regimes, that promote cluster-formation. More specifically, we consider various sensitivity functions for the individual oscillators, called the phase-response-curve [17, 22]. PRCs have been introduced, studied, and computed for many neuronal models [23, 24, 25, 22, 26]. They can serve as an appropriate control parameter determining the properties of the oscillators in the network [27]. In our paper, we restrict our analysis to PRCs, which turn to zero at the threshold, at which the oscillator emits a pulse. This choice is motivated by several well known neuron models [17, 22, 28] and means that the uncoupled system at the threshold is insensitive to small external perturbations.

Our work is accomplished by the bifurcation analysis of the cluster states and the analysis of the spectral properties of the completely synchronous state and eventually emerging two-cluster states. Our results reveals how the synchronization properties of the network depend on the PRC of the individual oscillators. We point out how the loss of stability of the synchronous solution may give rise to stable homoclinic connections of the synchronous solution and invariant two clusters. We derive conditions for the stability of these states and, in an exemplary family of unimodal, positive PRCs, we illustrate the mechanism by shifting the position of their maxima. For some range of the control parameter we observe a stable homoclinic connection of the synchronous solution, which leads to an apparent synchronization of the population with eventual beats out of perfect sync at a large time-scale, which are becoming more

rare with time. Thus, practically, a synchronized state is observed generically in such systems even in the case, when the completely synchronous state is locally unstable. For another range of parameters, we observe the stabilization of various two-cluster states, which bifurcate from the completely synchronous one-cluster state as predicted by the analytics. In the paper, the notions "complete synchronization" and "one-cluster" solution will be used interchangeably as they have the same meaning for our model.

The structure of the paper is as follows. In Sec. 2, the system is introduced. In Sec. 3, we reduce the dynamics to one-dimensional maps and in Sec. 4, we review the stability and bifurcations of the one-cluster state in this framework. We also explain how the existence of a stable homoclinic set may lead to the phenomenon of intermittent asymptotic synchronization. Appearance and stability of two-cluster states are studied in Sec. 5 and 6. Numerics for some illustrative example is shown in Sec. 7 and some technical details are included in the Appendix.

## 2 The system

Networks of weakly coupled oscillators can often be reduced to phase-models, which keep a single phase variable  $\varphi \in [0, 2\pi]$  for each oscillator [29, 22, 25]. In this reduction, one naturally encounters a function which measures the local sensitivity of an oscillator's phase to small perturbations – the phase response curve (PRC). If the perturbations act along only one direction of the state space, e. g. the voltage component in many neuron models, the PRC can be represented as a scalar function. Further reduction is possible when the coupling takes place on a considerably smaller time scale than the period of oscillations. In this case it is reasonable to approximate the interaction by an impact, i.e. by assuming that the interaction is immediate. By combining these two reductions, one obtains the model of pulse-coupled phase-oscillators [30, 17, 31, 27], which is the subject of our paper.

We consider the system of  $N$  identical phase-oscillators, whose dynamics are given as

$$\dot{\varphi}_j(t) = 1 + \frac{\kappa}{N} Z(\varphi_j(t)) \sum_{t_{kl}, k \neq j} \delta(t - t_{kl}), \quad j = 1, \dots, N. \quad (1)$$

Here  $t_{kl}$  are time moments when  $k$ -th oscillator reaches the threshold  $\varphi_k(t_{kl}) = 2\pi$ ,  $l = 1, 2, \dots$ . We call these time moments also "spikes". At this time, the  $k$ -th oscillator sends a spike and all other oscillators  $j$  with  $j \neq k$  obtain an impact

$$\varphi_j \mapsto \mu(\varphi_j) := \varphi_j + \frac{\kappa}{N} Z(\varphi_j), \quad (2)$$

where  $Z(\varphi)$  is the PRC. At the same time moment, the  $k$ -th oscillator resets to  $\varphi_k = 0$ . It is assumed that the

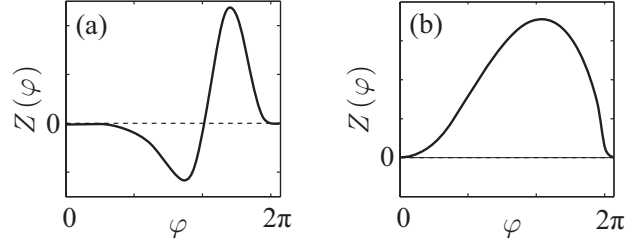


Figure 1: Examples of different PRCs. (a) Hodgkin-Huxley model, (b) Connor model. (adapted from [24]).

phase response curve  $Z(\varphi)$  is smooth inside  $(0, 2\pi)$ , but smoothness of derivatives in the endpoints is explicitly not assumed, i.e. possibly  $Z'(0) \neq Z'(2\pi)$ . Moreover, we assume  $Z(0) = Z(2\pi) = 0$ , which is frequently met in neuron models and means that a neuron is insensitive to external stimulation when it is generating or has just generated an action potential [17, 22, 28] (see Fig. 1).  $\kappa > 0$  is the coupling strength.

An obvious but important property of system (1) is that the order of the phases is invariant if the quotient  $\kappa/N$  of coupling strength and network size is sufficiently small. This means that the oscillators do not overrun each other with time. If

$$\frac{\kappa}{N} < \frac{1}{\left| \min_{\varphi \in [0, 2\pi]} Z'(\varphi) \right|}, \quad (3)$$

the map (2) becomes strictly monotonous and thus, the phase-ordering is preserved during spikes as well.

Although the dynamical system (1) together with the resetting condition is defined completely, it is worth to notice that it is equivalent to a discrete  $N$ -dimensional return map  $(\varphi_1, \dots, \varphi_N) \rightarrow K(\varphi_1, \dots, \varphi_N)$ . This return map can be obtained by fixing the position of one oscillator, e.g.  $\varphi_N = 0$ . Taking into account that the phase ordering is preserved, one iteration of the return map corresponds to one spike of each oscillator, i.e.  $N$  spikes altogether. More exact definition of the return map is given in Appendix 9.1.

Given (3), the synchronous solution

$$\varphi_1 = \dots = \varphi_N$$

is known to be linearly stable if and only if for all  $N_1 < N$  the following condition holds

$$\left| \left( 1 + \frac{\kappa}{N} Z'(0) \right)^{N-N_1} \left( 1 + \frac{\kappa}{N} Z'(2\pi) \right)^{N_1} \right| < 1. \quad (4)$$

This was proven in [17] by analyzing the linearization of the return-map. The terms in (4) are the eigenvalues of this linearization at its fixed point  $\varphi_1 = \dots = \varphi_N$ . Remarkably, for the case  $Z'(0) \neq Z'(2\pi)$ , there might be a loss of stability induced by an increasing of the population size.

### 3 Dynamics in invariant cluster subspaces

In this section, we study the dynamics of the return map in invariant subspaces  $\Pi_{N_1}$  of the form

$$\Pi_{N_1} = \left\{ \begin{array}{l} \varphi_1 = \dots = \varphi_{N_1} = \delta, \\ \varphi_{N_1+1} = \dots = \varphi_N = 0 \end{array} \middle| \delta \in (0, 2\pi) \right\}. \quad (5)$$

In these subspaces, the population is split into two clusters. The distance between those clusters is denoted by  $\delta$  (or  $2\pi - \delta$ ), which is the natural coordinate in  $\Pi_{N_1}$ . We can reduce the action of return map on  $\Pi_{N_1}$  as follows. Choose a particular initial state in  $\Pi_{N_1}$ , i.e.

$$\varphi_1 = \dots = \varphi_{N_1} = \delta \text{ and } \varphi_{N_1+1} = \dots = \varphi_N = 0,$$

with a particular initial distance  $\delta$ . Under the dynamics of (1), the next event in time will be the collective burst of the oscillators of the first cluster at time  $t = 2\pi - \delta$ . These are immediately resetted to  $\varphi = 0$ , i. e.

$$\varphi_1 = \dots = \varphi_{N_1} = 0.$$

The impact of the burst on an oscillator of the second cluster is obtained by repetitive application of the function  $\mu$  from (2) – one time for each oscillator in the first cluster. This leads to

$$\varphi_{N_1+1} = \dots = \varphi_N = \mu^{N_1}(2\pi - \delta),$$

where  $\mu^n$  denotes the  $n$ -fold superposition of the function  $\mu$ , i.e.  $\mu^n(\delta) = \underbrace{\mu(\mu(\dots \mu(\delta) \dots))}_n$ . At next, all oscillators

advance with equal velocity, until the second cluster reaches the threshold, that is,

$$\varphi_{N_1+1} = \dots = \varphi_N = 2\pi.$$

Accordingly the first cluster is located at

$$\varphi_1 = \dots = \varphi_{N_1} = 2\pi - \mu^{N_1}(2\pi - \delta).$$

The following burst of the second cluster completes the reduction of the return map and after the application of the return map, the new distance is given by

$$Y_{N_1}(\delta) = \mu^{N-N_1}(2\pi - \mu^{N_1}(2\pi - \delta)), \quad \delta \in [0, 2\pi]. \quad (6)$$

The one-dimensional map (6) determines completely the dynamics within the subspace  $\Pi_{N_1}$ , i.e. the dynamics of perfect two-clusters (5). Fig. 2 shows typical behaviors of these functions and corresponding cobweb-diagrams. A fixed point  $\delta_* \in (0, 2\pi)$  of this map correspond to a two-cluster fixed point of the global return map  $K$  or, equivalently, to a periodic two-cluster state of the original system

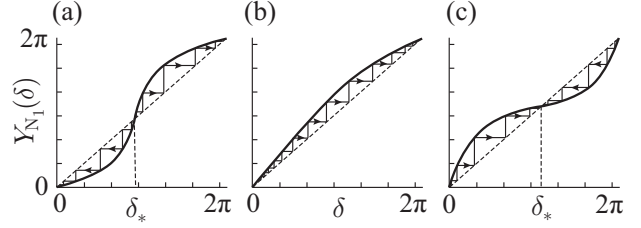


Figure 2: Cobweb-diagrams for the one-dimensional maps  $Y_{N_1}$  within the two-cluster subspaces  $\Pi_{N_1}$ . A fixed point  $\delta_* \in (0, 2\pi)$  corresponds to a stationary two-cluster state of the return map. Chart (a) shows a stable synchronous state and an unstable two-cluster state. In (b) one can observe a homoclinic connection of the synchronous state, resembled by a heteroclinic connection of  $\delta = 0$  and  $\delta = 2\pi$  under  $Y_{N_1}$ , and (c) shows an unstable synchronous state together with a two-cluster state, that is stable to perturbations in the subspace  $\Pi_{N_1}$ . Possible situations with several fixed points for  $Y_{N_1}$  are not shown. In Sec. 5, we explain, how the cases (a) and (b), resp. (b) and (c), are connected via the bifurcations of the synchronous solution.

(1). In general, the shape of  $Y_{N_1}(\delta)$  depends on the cluster sizes  $(N_1, N - N_1)$ , the PRC  $Z(\varphi)$ , and the coupling strength  $\varkappa$ .

In particular, these subspaces are of interest, since bifurcations along them govern the stability properties of the synchronous state, as we show in the next section.

### 4 Stability of the synchronous state

The trivial fixed points  $\delta = 0$  and  $\delta = 2\pi$  of  $Y_{N_1}$  correspond to the synchronous state. Derivatives of  $Y_{N_1}$  at these points can be computed as

$$\begin{aligned} Y'_{N_1}(0) &= \left(1 + \frac{\varkappa}{N} Z'(0)\right)^{N-N_1} \left(1 + \frac{\varkappa}{N} Z'(2\pi)\right)^{N_1}, \\ Y'_{N_1}(2\pi) &= \left(1 + \frac{\varkappa}{N} Z'(0)\right)^{N_1} \left(1 + \frac{\varkappa}{N} Z'(2\pi)\right)^{N-N_1} \\ &= Y'_{N-N_1}(0). \end{aligned} \quad (7)$$

Since the linearized dynamics of the cluster distance  $\delta$  for small  $\delta > 0$  is governed by

$$\delta \rightarrow Y'_{N_1}(0) \delta, \quad (8)$$

the derivatives  $Y'_{N_1}(0)$  are multipliers of the map governing its local stability at  $\delta = 0$ . Hence the linear stability conditions of the synchronous state  $\delta = 0$  under  $Y_n$  for  $n = 1, \dots, N - 1$  are  $|Y'_n(0)| < 1$ . These are identical to (4) because the invariant directions  $\varphi_1 = \dots = \varphi_{N_1} = 1$ ,  $\varphi_{N_1+1} = \dots = \varphi_N = 0$  are eigenvectors of the return map

at the synchronous solution  $\varphi_1 = \dots = \varphi_N = 0$ . It is evident, that the maximal multiplier of the linearized map (8) is either

$$Y'_1(0) = \left(1 + \frac{\kappa}{N} Z'(0)\right)^{N-1} \left(1 + \frac{\kappa}{N} Z'(2\pi)\right)$$

or

$$Y'_{N-1}(0) = \left(1 + \frac{\kappa}{N} Z'(0)\right)^1 \left(1 + \frac{\kappa}{N} Z'(2\pi)\right)^{N-1}$$

depending on the values of  $Z'(0)$  and  $Z'(2\pi)$ . This means, that the maximal growth of the cluster distance is observed in the case when only one oscillator is separated from the rest of the population, i.e.  $N_1 = 1$  or  $N_1 = N - 1$ .

When the number of oscillators  $N$  is large, one can obtain the approximation

$$Y'_{N_1}(0) \approx \exp[\kappa((1-p)Z'(0) + pZ'(2\pi))], \quad (9)$$

where  $p = N_1/N$  denotes the ratio of the oscillator number in the first cluster to the total number. This means that for large populations, the stability of the synchronous state to perturbations in form of two-clusters with  $N_1 = pN$  and  $N - N_1 = (1-p)N$  elements is governed by the condition

$$(1-p)Z'(0) + pZ'(2\pi) < 0 \quad (10)$$

and is independent on coupling strength  $\kappa$ . In particular, the synchronous solution is linearly stable for large populations only if both  $Z'(2\pi) < 0$  and  $Z'(0) < 0$ .

## 5 Two-cluster bifurcations of the synchronous state

In this section, we study generic codimension-1 bifurcations of the synchronous state, which lead to the emergence of various two-cluster states. We assume that the PRC is varied smoothly in some parameter  $\beta$ , that is,

$$Z(\varphi) = Z_\beta(\varphi).$$

In turn, the functions  $\mu(\varphi) = \mu(\varphi, \beta)$  and  $Y_{N_1}(\delta) = Y_{N_1}(\delta, \beta)$  become  $\beta$ -dependent, too. For the sake of readability, we will mostly omit this dependency in formulas. We still demand that  $Z_\beta(0) = Z_\beta(2\pi) = 0$  and that (3) is fulfilled with  $Z = Z_\beta$  for all  $\beta$ .

As seen in the previous section, the synchronous solution is linearly stable in the two-cluster subspace  $\Pi_{N_1}$  if and only if

$$\max\{\lambda_{N_1}(\beta), \lambda_{N-N_1}(\beta)\} < 1, \quad (11)$$

where

$$\begin{aligned} \lambda_n(\beta) &= Y'_n(0) = Y'_{N-n}(2\pi) \\ &= \left(1 + \frac{\kappa}{N} Z'_\beta(0)\right)^n \left(1 + \frac{\kappa}{N} Z'_\beta(2\pi)\right)^{N-n}. \end{aligned}$$

The loss of stability of the synchronous state in the subspace  $\Pi_{N_1}$  takes place if one of the multipliers  $\lambda_{N_1}(\beta)$  or  $\lambda_{N-N_1}(\beta)$  becomes bigger than 1 as  $\beta$  passes some critical value  $\beta_1$  with

$$\max\{\lambda_{N_1}(\beta_1), \lambda_{N-N_1}(\beta_1)\} = 1.$$

Such bifurcation causes the change of the form of the mapping  $Y_{N_1}$  from those shown in Fig. 2(a) to Fig. 2(b). Note that, generally, this loss is only one sided, giving the possibility of an emergence of a robust homoclinic connection to the synchronous solution as seen in Fig. 2(b). In a second bifurcation, the stability might be lost completely as  $\beta$  reaches a critical value  $\beta_2$  with

$$\min\{\lambda_{N_1}(\beta_2), \lambda_{N-N_1}(\beta_2)\} = 1.$$

If  $\beta_1 \neq \beta_2$ , there is either a creation or annihilation of a fixed point  $\delta_* = Y_{N_1}(\delta_*) \in (0, 2\pi)$  in each critical value of  $\beta$ . Note that, since  $Y'_n(2\pi) = Y'_{N-n}(0)$ , the bifurcation points  $\beta = \beta_c$  will coincide for  $N_1 = n$  and  $N_1 = N - n$ . The existence of a fixed point  $\delta_1$  of  $Y_{N_1}$  always implies that  $\delta_2 = \mu^{N_1}(2\pi - \delta_1)$  is a fixed point of  $Y_{N-N_1}$ . Therefore, the bifurcations appear as pitchfork bifurcations of the return map.

## 6 Stability of two-cluster states

In this section, we will provide explicit conditions for the stability of the two-cluster state

$$\varphi_1 = \dots = \varphi_{N_1} = \delta_*, \quad \varphi_{N_1+1} = \dots = \varphi_N = 0. \quad (12)$$

These conditions will be given by the formulas (20), (21), and (22). The practical usefulness of these conditions is illustrated later in Sec. 7 by determining the region in the parameter space with the coexisting stable two-cluster states. Recall, that the two-cluster solution (12) corresponds to a fixed point  $\delta_* = Y_{N_1}(\delta_*)$ .

Let us investigate the effect of small perturbations to (12). Because of the original system's symmetry with respect to index permutations, it suffices to consider perturbations which do not change the phase-order (see Appendix 9.1 and [17]). Here, these admissible perturbations are of the form

$$\begin{aligned} \eta &= (\eta_1, \dots, \eta_{N_1}, \eta_{N_1+1}, \dots, \eta_N), \\ \eta_1 &\geq \dots \geq \eta_{N_1} \geq 0, \quad \eta_{N_1+1} \geq \dots \geq \eta_N = 0. \end{aligned}$$

To avoid tedious calculations, we do not perform a full linearization of the return map and calculation of all multipliers. Instead, we will provide estimates, that are sharp for  $N \rightarrow \infty$ , for the largest multipliers in the following

invariant subspaces of admissible perturbations:

$$\begin{aligned}\mathcal{V}_1 &= \{(\eta_1, \dots, \eta_{N_1-1}, 0, \dots, 0) \mid \eta_1 \geq \dots \geq \eta_{N_1} = 0\}, \\ \mathcal{V}_2 &= \{(0, \dots, 0, \eta_{N_1+1}, \dots, \eta_{N-1}, 0) \mid \\ &\quad \eta_{N_1+1} \geq \dots \geq \eta_N = 0\}, \\ \mathcal{V}_3 &= \{(\eta_1, \dots, \eta_{N_1}, 0, \dots, 0) \mid \eta_1 = \dots = \eta_{N_1} = \delta \geq 0\}.\end{aligned}$$

Here,  $\mathcal{V}_1$  and  $\mathcal{V}_2$  contain *intra*-cluster perturbations, which only affect phases inside one cluster, and  $\mathcal{V}_3$  contains the perturbation of the cluster distance, i. e. the *inter*-cluster perturbations. Since the direct product of these invariant subspaces contains all admissible perturbations, the linear stability of the full system combines from stability in the subspaces.

Let us first turn to the intra-cluster perturbations in  $\mathcal{V}_1$  and  $\mathcal{V}_2$ . We introduce the cluster-widths for the state  $(\varphi_1, \dots, \varphi_N)$  as

$$W_1 = \varphi_1 - \varphi_{N_1} \text{ and } W_2 = \varphi_{N_1+1} - \varphi_N.$$

In the perfect two-cluster state (12) we have  $W_1 = W_2 = 0$ . If this state is perturbed along  $\mathcal{V}_1$ , the cluster-width of the first cluster becomes positive, i. e.  $W_1 = \eta_1$  and  $W_2 = 0$ . Analogously, perturbations along  $\mathcal{V}_2$  result in  $W_1 = 0$  and  $W_2 = \eta_{N_1+1}$ .

First, let us consider the perturbation within  $\mathcal{V}_1$  when the first cluster with  $N_1$  elements is perturbed. The intra-stability of one cluster is determined by the change of its width during one period, i.e. one application of the return map. These changes effectively take place only at two events, i. e. at the crossing of the threshold either by the first cluster itself or by the second cluster. Denote the maximal possible change of the width of the perturbed cluster during its own crossing as  $\Delta_1^{N_1}(\varepsilon)$ , where  $\varepsilon \geq 0$  is the width before the burst. This is, an initial width  $\varepsilon$  results in a new width  $\varepsilon + \Delta_1^{N_1}(\varepsilon)$  after the burst. Since the other cluster is not involved in this process, we can treat it as a burst of a single cluster in a system of  $N_1$  oscillators. Sections 4 and 5 showed that, the maximal  $\Delta_1^{N_1}(\varepsilon)$  is realized either by the perturbation  $\varepsilon = \eta_1 > \eta_2 = \dots = \eta_{N_1} = 0$  or by  $\varepsilon = \eta_1 = \dots = \eta_{N_1-1} > \eta_{N_1} = 0$ , depending on the values of  $Z'(0)$  and  $Z'(2\pi)$ .

Similarly, we denote changes of the cluster's width at the crossing of the other cluster as  $\Delta_2^{N-N_1}(\varepsilon)$ , where  $\varepsilon \geq 0$  is as before and  $N - N_1$  is the number of elements in the other, unperturbed cluster. Note that  $\Delta_2^{N-N_1}(\varepsilon)$  is the same for all intra-cluster perturbations of magnitude  $\varepsilon$ , since the phase order is preserved and solely the distance between the first and the last phases  $\varphi_1 - \varphi_{N_1}$  in the cluster matters.

The maximal width for perturbations of the first cluster after one return is then

$$W_1(\varepsilon) = \varepsilon + \Delta_1^{N_1}(\varepsilon) + \Delta_2^{N-N_1}(\varepsilon + \Delta_1^{N_1}(\varepsilon))$$

with  $\varepsilon = \eta_1$ .

Similarly, the width of the second cluster (within the invariant subspace  $\mathcal{V}_2$ ) changes as

$$W_2(\varepsilon) = \varepsilon + \Delta_2^{N_1}(\varepsilon) + \Delta_1^{N-N_1}(\varepsilon + \Delta_2^{N_1}(\varepsilon)),$$

for  $\varepsilon = \eta_{N_1+1}$ . Stability conditions with respect to all possible intra-cluster perturbations (within the subspace  $\mathcal{V}_1 \oplus \mathcal{V}_2$ ) are then given by  $W_1'(0) < 1$  and  $W_2'(0) < 1$ , i. e.

$$\begin{aligned}W_1'(0) &= 1 + \left(\Delta_1^{N_1}\right)'(0) + \left(\Delta_2^{N-N_1}\right)'(0) \\ &\quad + \left(\Delta_2^{N-N_1}\right)'(0) \cdot \left(\Delta_1^{N_1}\right)'(0) < 1, \quad (13)\end{aligned}$$

$$\begin{aligned}W_2'(0) &= 1 + \left(\Delta_2^{N_1}\right)'(0) + \left(\Delta_1^{N-N_1}\right)'(0) \\ &\quad + \left(\Delta_1^{N-N_1}\right)'(0) \cdot \left(\Delta_2^{N_1}\right)'(0) < 1. \quad (14)\end{aligned}$$

The stability analysis of the synchronous solution in sections 4 and 5, applied to a population of  $n$  ( $n = N_1$  or  $n = N - N_1$ ) oscillators, implies that  $\Delta_1^n(\varepsilon)$  satisfies

$$\begin{aligned}1 + \left(\Delta_1^n\right)'(0) &= \left(1 + \frac{\kappa}{N} \min(Z'(0), Z'(2\pi))\right)^1 \\ &\quad \times \left(1 + \frac{\kappa}{N} \max(Z'(0), Z'(2\pi))\right)^{n-1},\end{aligned}$$

see (7). For large populations, this reads

$$1 + \left(\Delta_1^n\right)'(0) \approx \exp(\kappa p \max(Z'(0), Z'(2\pi))), \quad (15)$$

where  $p = n/N$ . This is obtained as in (9). The change of the width of a perturbed cluster at position  $\varphi = \delta$ , that is induced by the burst of another unperturbed cluster is given as (see Appendix 9.2 for details)

$$\Delta_2^n(\varepsilon) = \sum_{k=0}^{n-1} \frac{\kappa}{N} (Z(\mu^k(\delta + \varepsilon)) - Z(\mu^k(\delta))). \quad (16)$$

Hence,

$$\left(\Delta_2^n\right)'(0) = \sum_{k=0}^n \frac{\kappa}{N} Z'(\mu^k(\delta)) (\mu^k)'(\delta). \quad (17)$$

One can approximate (see Appendix 9.2) this sum in the limit  $N \rightarrow \infty$  by a simpler expression using the solution  $\vartheta(r, \varphi)$  to the initial value problem

$$\begin{aligned}\frac{\partial \vartheta}{\partial r}(r, \varphi) &= \kappa Z(\vartheta(r, \varphi)), \\ \vartheta(0, \varphi) &= \varphi.\end{aligned} \quad (18)$$

As argued in the Appendix 9.2, the function  $\vartheta(r, \varphi)$  is a smooth approximation of  $\mu^{r \cdot N}(\varphi)$ . Using this, we get

$$\left(\Delta_2^n\right)'(0) \approx \frac{Z(\vartheta(p, \delta)) - Z(\delta)}{Z(\delta)}, \quad (19)$$

where  $p = n/N$  and  $\delta$  is the position of the perturbed cluster, when the unperturbed cluster crosses the threshold.

Using (13), (15) and (19), we obtain for the two-cluster state (12) of large populations

$$W'_1(0) \approx \exp(\kappa p \max(Z'(0), Z'(2\pi))) \times \left(1 + \frac{Z(\delta_*) - Z(2\pi - \vartheta(p, 2\pi - \delta_*))}{Z(2\pi - \vartheta(p, 2\pi - \delta_*))}\right),$$

where  $p = N_1/N$ . That is, the condition for the intra-stability of the first cluster, (13), leads to:

$$\exp(\kappa p \max(Z'(0), Z'(2\pi))) \times \left(1 + \frac{Z(\delta_*) - Z(2\pi - \vartheta(p, 2\pi - \delta_*))}{Z(2\pi - \vartheta(p, 2\pi - \delta_*))}\right) < 1, \quad (20)$$

and for the second cluster, (14) reads

$$\exp(\kappa(1-p) \max(Z'(0), Z'(2\pi))) \times \left(1 + \frac{Z(\vartheta(p, 2\pi - \delta_*)) - Z(2\pi - \delta_*)}{Z(2\pi - \delta_*)}\right) < 1. \quad (21)$$

The stability of perturbations in  $\mathcal{V}_3$ , i. e. of the cluster distance, corresponds to the stability of the cluster position  $\delta_*$  as a fixed point of  $Y_{N_1}$ , i. e.  $|Y'_{N_1}(\delta_*)| < 1$ . For  $N \rightarrow \infty$ , this condition can be rewritten as

$$\frac{Z(\delta_*) \cdot Z(\vartheta(p, 2\pi - \delta_*))}{Z(2\pi - \vartheta(p, 2\pi - \delta_*)) \cdot Z(2\pi - \delta_*)} < 1. \quad (22)$$

For more details see Appendix 9.2.

Note that, for  $\kappa \rightarrow 0$ , i. e. very weak coupling, we can simplify (20)–(22) to

$$(1-p)Z'(\delta_0) + p \max(Z'(0), Z'(2\pi)) < 0, \quad (23)$$

$$pZ'(2\pi - \delta_0) + (1-p) \max(Z'(0), Z'(2\pi)) < 0, \quad (24)$$

$$p \cdot Z'(2\pi - \delta_0) + (1-p)Z'(\delta_0) < 0, \quad (25)$$

where  $\delta_0 = \lim_{\kappa \rightarrow 0} \delta_*$  – see Appendix 9.3. These latter conditions match exactly the conditions, that were obtained by Hansel et. al. in [32] for the linear stability in the averaged model

$$\dot{\varphi}_i(t) = 1 + \frac{\kappa}{N} \sum_{j=1}^N Z(\varphi_i(t) - \varphi_j(t)).$$

As in the averaged model, in the pulse-coupled case it is possible to encounter multistability in between stable cluster-states and the stable synchronous solution.

## 6.1 A special case

Let us now consider the situation

$$Z'(0) = Z'(2\pi) = 0. \quad (26)$$

This might seem degenerate, but in neuron models as well as in experimental neurophysiology, this property is not unusual – review the examples in Fig. 1 and note that the derivatives are indeed zero at  $\varphi = 0$  and  $\varphi = 2\pi$ . We picked a simple example of this kind to illustrate our results numerically in the Sec. 7. Given (26), formula (4) does not supply any information about the stability of the synchronous solution, because one finds that for arbitrary  $N_1$ ,

$$\left(1 + \frac{\kappa}{N} Z'(0)\right)^{N_1} \left(1 + \frac{\kappa}{N} Z'(2\pi)\right)^{N-N_1} = 1$$

and all multipliers are degenerate and equal to 1. Since the linear stability analysis does not provide any results, one must consider terms of higher order to complete a stability analysis for this case. We will go one step in this direction by investigating the nonlinear stability of the synchronous solution along the invariant split states as (5) and point out that similar mechanisms may participate in a destabilization as in the previous section. Consider quadratic terms along the split directions. One finds:

$$Y''_{N_1}(0) = (N - N_1) \frac{\kappa}{N} Z''(0) - N_1 \frac{\kappa}{N} Z''(2\pi), \quad (27)$$

$$Y''_{N_1}(2\pi) = (N - N_1) \frac{\kappa}{N} Z''(2\pi) - N_1 \frac{\kappa}{N} Z''(0) = -Y''_{N-N_1}(0). \quad (28)$$

Up to the leading terms, the dynamics governing small distances between two-clusters is given now by

$$\delta \rightarrow \delta + \frac{1}{2} Y''_{N_1}(0) \delta^2,$$

instead of (8). Thus, we have an analogous situations as in Sec. 5, Fig. 2. The synchronous state is stable under conditions

$$Y''_{N_1}(0) < 0, \quad Y''_{N_1}(2\pi) > 0.$$

Bifurcations from stable synchronous state to two-cluster-states occur in the same way as before. The conditions for the stability of two-cluster states (20)–(21) from Sec. 6 reduce to

$$\frac{Z(\delta_*)}{Z(2\pi - \vartheta(p, 2\pi - \delta_*))} < 1 \text{ and } \frac{Z(\vartheta(p, 2\pi - \delta_*))}{Z(2\pi - \delta_*)} < 1, \quad (29)$$

and imply (22) in the present case. Once more, for weak coupling, these conditions takes a simpler form, that is

$$Z'(\delta_0) < 0 \text{ and } Z'(2\pi - \delta_0) < 0, \quad (30)$$

where  $\delta_0 = \lim_{\kappa \rightarrow 0} \delta_*$ .

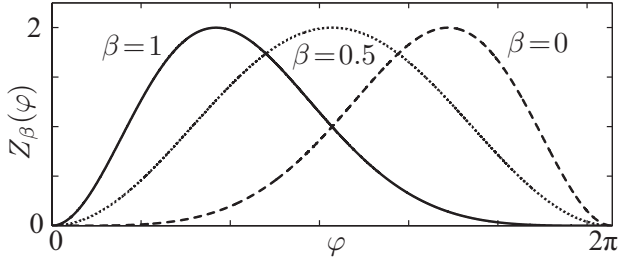


Figure 3: Family of unimodal PRCs  $Z_\beta(\varphi)$  that were used in simulations, see (33).

## 7 Numerics

In this section we provide a simple example, where branches of initially unstable two-clusters emerge and eventually stabilize for increasing  $\beta$ , as predicted by our analytics (see Fig. 6). Moreover, we will illustrate the stable homoclinic structure leading to intermittent synchronization (see Fig. 5).

In order to detect the appearance of one- or two-cluster states, we compute the order parameters

$$R_1(t) = \left| \frac{1}{N} \sum_{j=1}^N e^{i\varphi_j(t)} \right| \quad (31)$$

and

$$R_2(t) = \left| \frac{1}{N} \sum_{j=1}^N e^{i2\varphi_j(t)} \right|. \quad (32)$$

A perfect one-cluster state is characterized by  $R_1 = R_2 = 1$  and a perfect antiphase two-cluster is characterized by  $R_1 = 0$  and  $R_2 = 1$ . We present results of simulations for  $\kappa = 0.5$ , but qualitatively we observe similar behavior for a broad range of  $\kappa > 0$ .

Consider the following family of PRCs (see Fig. 3):

$$Z_\beta(\varphi) = 1 - \cos(\chi_\beta(\varphi)), \text{ for } \beta \in [0, 1], \quad (33)$$

$$\chi_\beta(\varphi) = \frac{(1-2\beta)}{2\pi}\varphi^2 + 2\beta\varphi.$$

As shown in Fig. 4, we observe two qualitatively different types of behavior depending on parameter  $\beta$ . For  $\beta < 0.5$ , i.e. when the maximum of the PRC is shifted to the right (see Fig. 3), the one-cluster state acts attracting on most initial states; for  $\beta > 0.5$  the maximum of the PRC is shifted to the left and two-cluster states become attracting. We have chosen initial conditions in a vicinity of a two-cluster state in Fig. 4(a) and (b), therefore the initial values of the order parameters are  $R_1 \approx 0$  and  $R_2 \approx 1$ . Figure 4(b) shows how the instability of the two-cluster state implies desynchronization transient, after

which the system is attracted to a synchronous one-cluster state. Similar behavior occurs for other initial conditions. Figure 4(c) and (d) illustrate the order parameters behavior for initial conditions close to the splay state (a state, where the phases are distributed). The initial values for the order parameters in the splay state are close to zero, but after a transient, they approach again the same asymptotic values as in (a) and (b).

A more complicated behavior occurs for the intermediate value of the parameter  $\beta = 0.5$ , i.e. when the PRC is symmetric. In this case, the order parameters  $R_1(t)$  and  $R_2(t)$  do not approach some asymptotic constant values but remain periodic in time. As a result, the maximum asymptotic values of both  $R_1$  and  $R_2$  do not coincide with the corresponding minimum values. This type of behavior is observed for a very small parameter interval of magnitude  $O(\frac{1}{N})$  around  $\beta \approx 0.5$ . It is worth mentioning, that  $Z_{0.5}(\varphi) = 1 - \cos(\varphi)$  was proposed as PRC for oscillators near a saddle-node bifurcation on a periodic orbit [24, 22]. Since  $\beta = 0.5$  is a critical value for our model, we advise caution for treating this case as exemplary in investigations. Figure 4 (e) and (f) summarize the behavior of the order parameters for different  $\beta$ .

### 7.1 Cluster-stability

Since  $Z'_\beta(0) = Z'_\beta(2\pi) = 0$ , for all  $\beta \in [0, 1]$ , we have

$$Y'_{\beta, N_1}(0) = Y'_{\beta, N_1}(2\pi) = 1, \text{ for all } N_1 = 1, \dots, N-1.$$

This means, expressions (27) and (28) become relevant to stability of the synchronous solutions. In our example, they read

$$Y''_{\beta, N_1}(0) = 4\kappa \left( (1-p)\beta^2 - p(1-\beta)^2 \right),$$

$$Y''_{\beta, N_1}(2\pi) = 4\kappa \left( (1-p)(1-\beta)^2 - p\beta^2 \right),$$

where  $p = N_1/N$ . For large populations, the synchronous solution is unstable for any  $\beta$ . Nevertheless, numerics show an attraction to the synchronous state, which can be explained by the existence of a stable homoclinic connection of the one-cluster ([33], see Fig. 5).

At  $\beta \approx 0.5$ , the symmetric two-cluster state gains stability and subsequently, with increasing  $\beta$ , asymmetric cluster-states emerge when  $Y''_{\beta, N_1}(0)$  changes sign and gain stability when (29) is fulfilled. The analytic predictions from Sec. 6 match the numerical results. More specifically, in Fig. 6(a) one observes pitchfork bifurcations of the synchronous state ( $\delta = 0$ ) leading to the appearance of two-cluster states. These two-cluster states are initially unstable but, with increasing  $\beta$ , they gain stability creating a large set of coexisting stable two-clusters. Figure 6(b) shows the stable clusters versus  $\beta$ . Solid line corresponds to the analytically predicted stability domain (29) and the dots are observed clusters from numerical calculations.

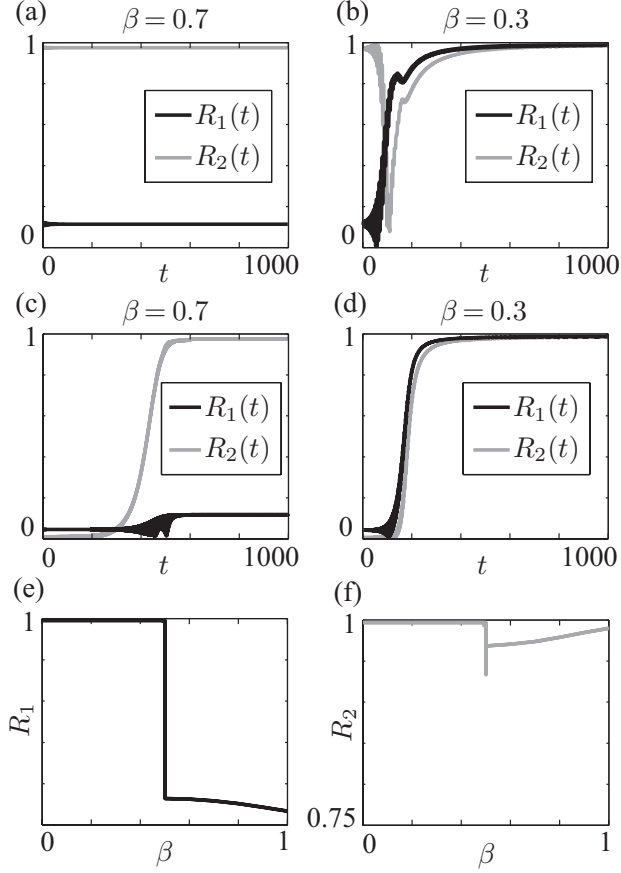


Figure 4: Asymptotic behavior of the order parameters. Charts (a) and (b) show  $R_1(t)$  and  $R_2(t)$  for a trajectory starting in a vicinity of the two-cluster state. The middle panel (c) and (d) belong to a trajectories starting in a vicinity of the splay state. Left charts (a) and (c) correspond to the parameter value  $\beta = 0.7$ , where the two-cluster state is attracting and (b) and (d) to  $\beta = 0.3$ , where one-cluster state is attracting. In (e) and (f): dependence of the asymptotic values for the order parameter  $R_1$  and  $R_2$  on  $\beta$ . For the most values of  $\beta$ , except  $\beta = 0.5$ , the order parameters tend to some constant value, when initialized near the splay state or the symmetric two-cluster state.

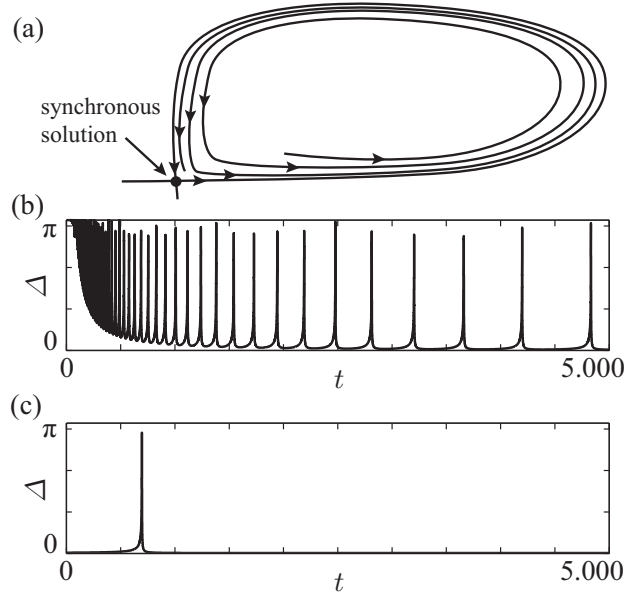


Figure 5: Homoclinic connection of the one-cluster. In (a): Synchronous solution (i.e. one-cluster state) as a saddle point in the phase space with a homoclinic loop. In (b) and (c): Width of the cluster  $\Delta(t) = \max_{1 \leq i, j \leq N} \{|\varphi_i(t) - \varphi_j(t)|\}$  as a function of time. Chart (a) shows the behavior along the orbit started at an initial condition close to the splay state (far from the one-cluster) and (b) shows the behavior along the orbit started close to a split-state with homoclinic connection as in Fig. 2 (b). The growing intervals between peaks in (a) indicate the existence of a stable homoclinic orbit.

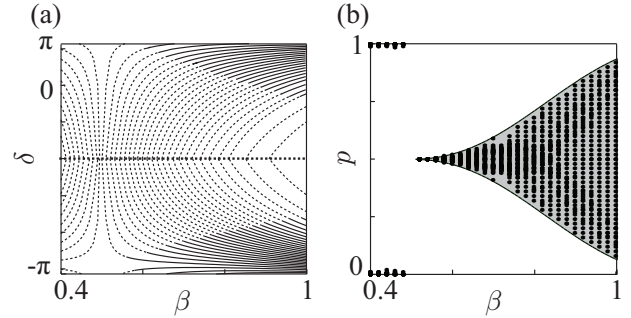


Figure 6: Stability and existence of two-cluster states. (a) A cascade of pitchfork bifurcations gives birth to fixed points of  $Y_{N_1}$  and  $Y_{N-N_1}$ . Solid lines denote stable two-cluster stationary states and dashed - unstable. The lines are shown only for selected values of  $p = N_1/N$ . Markers in Fig. (b) shows which two-clusters are stable in dependence on  $\beta$  and  $p$  (observed numerically). The value  $p = 0.5$  corresponds to the symmetric cluster and  $p \neq 0.5$  to non-symmetric clusters. The shaded region in (b) indicates the analytic prediction for the stability of the two-cluster states by (29).

## 8 Discussion

In this paper, we have considered the following question: How the individual properties of oscillators in a globally coupled system influence the formations of one- and two-cluster states? Working in the framework of pulse-coupled oscillators, the adjustable parameter for our study was chosen to be the PRC.

Starting from the results of Goel and Ermentrout [17] about the stability of one-cluster state, we have extended these results to the case when the first derivatives of the PRC at the threshold equal to zero. We have derived a one-dimensional map that describes the dynamics in invariant subspaces corresponding to various two-cluster states. By means of this map we identified pitchfork bifurcations of the one-cluster state, which lead to the emergence of periodic two-cluster states. For large populations, we provide explicit conditions for the linear stability of these states. The analysis of the one-dimensional map also reveals that a homoclinic connection to the synchronous one-cluster state is generic in the considered class of systems. Moreover, numerical analysis shows that a set of homoclinic connections can be globally attracting.

For the numerical illustration, we have chosen systems with positive, unimodal PRCs, which turn to zero at the threshold together with its first derivatives. This corresponds to the excitatory coupling. By varying the shape of this PRCs, we observe how the initially globally attracting one-cluster undergoes a sequence of bifurcations in which two-cluster states emerge and later on stabilize. This leads to the coexistence of multiple stable two-cluster states. The latter phenomenon resembles qualitatively the Eckhaus phenomenon [34, 35].

## Acknowledgments

This work was supported by Deutsche Forschungsgemeinschaft in the framework of SFB910 under the project A3 (L.L.) and Research Center Matheon under the project D21 (S.Y.).

## 9 Appendix

### 9.1 Formal definition of the return map

In this section, we derive the discrete return map for the system (1). Let us introduce the state-spaces

$$X_j = \{(\varphi_1, \dots, \varphi_N) \in [0, 2\pi] \mid \varphi_{[1+j]} \geq \dots \geq \varphi_{[N+j]} = 0\},$$

where  $[n] = n \bmod N$ . In particular

$$X_N = X_0 = \{(\varphi_1, \dots, \varphi_N) \in [0, 2\pi] \mid \varphi_1 \geq \dots \geq \varphi_N = 0\}.$$

Since all oscillators are taken to be identical and homogeneously coupled, the system is symmetric with respect to permutations of indexes ( $\mathfrak{S}_N$ -symmetry). Therefore, without loss of generality, let us consider initial states in  $X_0$ . The return map  $K : X_0 \mapsto X_0$  is composed of  $N$  maps  $k_j : X_{j-1} \mapsto X_j$ ,  $j = 1, \dots, N$ , defined as

$$k_j(\varphi_1, \dots, \varphi_j, \dots, \varphi_N) := \left( \varphi_1 + 2\pi - \varphi_j + \frac{\kappa}{N} Z(\varphi_1 + 2\pi - \varphi_j), \dots, \varphi_N + 2\pi - \varphi_j + \frac{\kappa}{N} Z(\varphi_N + 2\pi - \varphi_j) \right).$$

where the  $j$ -th The map  $k_j$  describes the firing of the  $j$ -th oscillator, assuming it has maximal phase. Under the assumption that the phase order is preserved, i.e. (3) holds, the return map is given by

$$K = k_N \circ \dots \circ k_1 : X_0 \rightarrow X_1 \rightarrow \dots \rightarrow X_N = X_0.$$

Note that each  $k_j$  is smooth. Linearizations of  $K$  capture perturbations, which keep the presumed phase-ordering. Because of the system's symmetry, it suffices to consider these for a determination of linear stability (see also [17]).

### 9.2 Approximation of repetitive firing

Assume that (3) holds. Then, the phase order is preserved. Consider a perturbed cluster,  $\varphi_1 \geq \dots \geq \varphi_{N_1}$ , with  $N_1 = p \cdot N$  and

$$\varphi_1 = \delta + \varepsilon, \quad \varphi_{N_1} = \delta.$$

The change of the width of this cluster during the threshold crossing of another unperturbed cluster

$$\varphi_{N_1+1} = \dots = \varphi_N = 2\pi$$

with  $N_2 = (1-p)N$  oscillators is given by the change of the distance between the leading oscillator  $\varphi_1$  and the last oscillator  $\varphi_{N_1}$ . The new position  $\varphi_j^+$  of a single oscillator  $\varphi_j$  of the perturbed cluster is given as

$$\begin{aligned} \varphi_j^+ &= \mu^{N_2}(\varphi_j) = \underbrace{\mu(\mu(\dots \mu(\varphi_j) \dots))}_{N_2} \\ &= \varphi_j + \sum_{k=0}^{N_2-1} \frac{\kappa}{N} Z(\mu^k(\varphi_j)). \end{aligned}$$

Thus, the change of width of the perturbed cluster is

$$\begin{aligned} \varphi_1^+ - \varphi_{N_1}^+ &= \left( \varepsilon + \delta + \sum_{k=0}^{N_2-1} \frac{\kappa}{N} Z(\mu^k(\delta + \varepsilon)) \right) \\ &\quad - \left( \delta + \sum_{k=0}^{N_2-1} \frac{\kappa}{N} Z(\mu^k(\delta)) \right) \\ &= \varepsilon + \sum_{k=0}^{N_2-1} \frac{\kappa}{N} (Z(\mu^k(\delta + \varepsilon)) - Z(\mu^k(\delta))). \end{aligned}$$

In this way, we arrive at (16).

Let us introduce a function,  $\vartheta : [0, 1] \times [0, 2\pi] \rightarrow [0, 2\pi]$ , that approximates the iterations of  $\mu$  as follows:

$$\vartheta(r, \varphi) \approx \mu^k(\varphi), \text{ for } r = \frac{k}{N}.$$

Then,

$$\begin{aligned} \vartheta\left(r + \frac{1}{N}, \varphi\right) - \vartheta(r, \varphi) &\approx \mu^{r \cdot N + 1}(\varphi) - \mu^{r \cdot N}(\varphi) \\ &= \frac{\varkappa}{N} Z(\mu^{r \cdot N}(\varphi)) \\ &\approx \frac{\varkappa}{N} Z(\vartheta(r, \varphi)), \end{aligned}$$

or equivalently,

$$\frac{\vartheta\left(r + \frac{1}{N}, \varphi\right) - \vartheta(r, \varphi)}{1/N} \approx \varkappa Z(\vartheta(r, \varphi)).$$

Therefore, for large  $N$ ,  $\vartheta(r, \varphi)$  is a solution to the initial value problem (18). Further,  $\frac{\partial \vartheta}{\partial \varphi}(r, \varphi)$  solves the linear system

$$\begin{aligned} \frac{\partial}{\partial r} \frac{\partial \vartheta}{\partial \varphi}(r, \varphi) &= \varkappa Z'(\vartheta(r, \varphi)) \frac{\partial \vartheta}{\partial \varphi}(r, \varphi), \\ \frac{\partial \vartheta}{\partial \varphi}(0, \varphi) &= 1. \end{aligned}$$

Therefore,

$$\frac{\partial \vartheta}{\partial \varphi}(r, \varphi) = \exp\left(\int_0^r \varkappa Z'(\vartheta(s, \varphi)) ds\right).$$

Taking into account the property (18), we obtain

$$\frac{\partial \vartheta}{\partial \varphi}(r, \varphi) = \exp\left(\int_{\varphi}^{\vartheta(r, \varphi)} \frac{Z'(\theta)}{Z(\theta)} d\theta\right) = \frac{Z(\vartheta(r, \varphi))}{Z(\varphi)}. \quad (34)$$

Now, we can simplify the expression (17) by means of  $\vartheta$ . For this, we substitute  $\mu^k(\varphi)$  by  $\vartheta(\frac{k}{N}, \varphi)$  and the sum over  $k$  by an integral over  $r$  in (17). As a result, we obtain

$$\begin{aligned} &\sum_{k=0}^{N_2-1} \frac{\varkappa}{N} Z'(\mu^k(\delta)) (\mu^k)'(\delta) \\ &\approx \int_0^{1-p} \varkappa Z'(\vartheta(r, \delta)) \frac{d\vartheta}{d\varphi}(r, \delta) dr \\ &= \frac{Z(\vartheta(1-p, \delta)) - Z(\delta)}{Z(\delta)}. \end{aligned}$$

Thus, for large populations, (17) leads to (19).

The inter-cluster-stability is given by the stability of  $\delta_*$  as a fixed point of  $Y_{p \cdot N}$ , that is,  $|Y'_{p \cdot N}(\delta_*)| < 1$ . In terms of  $\vartheta(r, \varphi)$ , we have  $Y_{p \cdot N}(\delta) \approx \vartheta(1-p, 2\pi - \vartheta(p, 2\pi - \delta))$  and fixed points  $\delta_* = Y_{p \cdot N}(\delta_*)$  satisfy  $\delta_* \approx \vartheta(1-p, 2\pi - \vartheta(p, 2\pi - \delta_*))$ . Thereby one obtains (22).

### 9.3 Weak coupling in large populations

Assume that for sufficiently small  $\varkappa$ , there exist fixed points  $\delta(\varkappa) = Y_{p \cdot N}(\delta(\varkappa), \varkappa)$ , with  $p \cdot N \in \{1, \dots, N\}$ . Further, assume that the limit  $\delta_0 = \lim_{\varkappa \rightarrow 0} \delta(\varkappa)$  exists. Actually, it is a generic property for any point  $\delta_0 \in (0, 2\pi)$ , that fulfills  $(1-p)Z(\delta_0) = pZ(2\pi - \delta_0)$ , that there exists a family of fixed points of  $Y_{p \cdot N}$  with  $\delta_0 = \lim_{\varkappa \rightarrow 0} \delta(\varkappa)$ .

For small  $\varkappa$ , the linearization of (20)–(22) in  $\varkappa = 0$  gives the stability conditions (23)–(25). For example, the linearization of (20) is

$$\begin{aligned} 0 &> \frac{\partial}{\partial \varkappa} \left( \exp(\varkappa p \max(Z'(0), Z'(2\pi))) \right. \\ &\quad \times \left. \left( 1 + \frac{Z(\delta_*) - Z(2\pi - \vartheta(p, 2\pi - \delta_*))}{Z(2\pi - \vartheta(p, 2\pi - \delta_*))} \right) \right) \quad (35) \end{aligned}$$

In the following, we add  $\varkappa$  explicitly as an argument where needed. Note that the two-cluster fixed points  $\delta_* = \delta(\varkappa)$  are  $\varkappa$ -dependent as well as the function  $\vartheta(r, \varphi) = \vartheta(r, \varphi, \varkappa)$  from the previous section and  $Y_{p \cdot N}(\varphi) = Y_{p \cdot N}(\varphi, \varkappa)$ . Using (18), we obtain  $\frac{\partial \vartheta}{\partial \varkappa}(0, \varphi, \varkappa)$  as a solution to

$$\begin{aligned} \frac{\partial}{\partial r} \frac{\partial \vartheta}{\partial \varkappa}(r, \varphi, \varkappa) &= Z(\vartheta(r, \varphi, \varkappa)) \\ &\quad + \varkappa Z'(\vartheta(r, \varphi, \varkappa)) \frac{\partial \vartheta}{\partial \varkappa}(r, \varphi, \varkappa), \\ \frac{\partial \vartheta}{\partial \varkappa}(0, \varphi, \varkappa) &= 0. \end{aligned}$$

This can be solved explicitly as

$$\frac{d\vartheta}{d\varkappa}(r, \varphi, \varkappa) = r \cdot Z(\vartheta(r, \varphi, \varkappa)). \quad (36)$$

Using  $\vartheta(r, \varphi, 0) = \varphi$ , (34) and (36), the condition (35) in  $\varkappa = 0$  becomes

$$\begin{aligned} 0 &> p \max(Z'(0), Z'(2\pi)) \\ &\quad + \frac{\partial}{\partial \varkappa} \left( \frac{Z(\delta(\varkappa)) - Z(2\pi - \vartheta(p, 2\pi - \delta(\varkappa), \varkappa))}{Z(2\pi - \vartheta(p, 2\pi - \delta(\varkappa), \varkappa))} \right) \\ &= p \max(Z'(0), Z'(2\pi)) + \frac{pZ(2\pi - \delta_0)Z'(\delta_0)}{Z(\delta_0)}. \quad (37) \end{aligned}$$

Differentiation of the fixed point equation  $\delta(\varkappa) = Y_{p \cdot N}(\delta(\varkappa), \varkappa) \approx \vartheta(1-p, 2\pi - \vartheta(p, 2\pi - \delta(\varkappa), \varkappa))$  in  $\varkappa = 0$  yields

$$0 \approx (1-p)Z(\delta_0) - pZ(2\pi - \delta_0). \quad (38)$$

Inserting this into (37) gives (23). Similarly, one obtains (24) from (21) and (25) from (22).

## References

- [1] A. Pikovsky, M. Rosenblum, J. Kurths, Synchronization. A Universal Concept in Nonlinear Sciences, Cambridge University Press, 2001.
- [2] S. H. Strogatz, Exploring complex networks, *Nature* 410 (2001) 268 – 276.
- [3] H.-J. Wünsche, S. Bauer, J. Kreissl, O. Ushakov, N. Korneyev, F. Henneberger, E. Wille, H. Erzgräber, M. Peil, W. Elsässer, I. Fischer, Synchronization of delay-coupled oscillators: A study of semiconductor lasers, *Phys. Rev. Lett.* 94 (2005) 163901–1–163901–4.
- [4] I. Fischer, R. Vicente, J. M. Buldú, M. Peil, C. R. Mirasso, M. C. Torrent, J. Garcia-Ojalvo, Zero-lag long-range synchronization via dynamical relaying, *Phys. Rev. Lett.* 97 (2006).
- [5] S. Yanchuk, K. R. Schneider, L. Recke, Dynamics of two mutually coupled semiconductor lasers: Instantaneous coupling limit, *Phys. Rev. E* 69 (2004) 056221–1–056221–12.
- [6] S. Yanchuk, A. Stefanski, T. Kapitaniak, J. Wojewoda, Dynamics of an array of coupled semiconductor lasers, *Phys. Rev. E* 73 (2006) 016209–1–016209–7.
- [7] K. M. Cuomo, A. V. Oppenheim, Circuit implementation of synchronized chaos with applications to communications, *Phys. Rev. Lett.* 71 (1993) 65–68.
- [8] I. Kanter, E. Kopelowitz, W. Kinzel, Public channel cryptography: Chaos synchronization and hilbert’s tenth problem, *Phys. Rev. Lett.* 101 (2008) 084102.
- [9] E. Mosekilde, Y. Maistrenko, D. Postnov, Chaotic Synchronization. Application to Living Systems., World Scientific, 2002.
- [10] P. Perlikowski, A. Stefanski, T. Kapitaniak, 1:1 mode locking and generalized synchronization in mechanical oscillators, *Journal of Sound and Vibration* 318 (2008) 329 – 340.
- [11] P. Perlikowski, S. Yanchuk, M. Wolfrum, A. Stefanski, P. Mosiolek, T. Kapitaniak, Routes to complex dynamics in a ring of unidirectionally coupled systems, *Chaos* 20 (2010) 013111.
- [12] P. Tass, Phase Resetting in Medicine and Biology. Stochastic Modelling and Data Analysis, Springer Series in Synergetics, Springer, 1999.
- [13] M. Timme, T. Geisel, F. Wolf, Speed of synchronization in complex networks of neural oscillators: Analytic results based on random matrix theory, *Chaos* 16 (2006) 015108.
- [14] O. V. Popovych, C. Hauptmann, P. A. Tass, Control of neuronal synchrony by nonlinear delayed feedback., *Biol Cybern* 95 (2006) 69–85.
- [15] R. Elble, W. Koller, Tremor, The John Hopkins University Press, 1990.
- [16] P. Tass, A model of desynchronizing deep brain stimulation with a demand-controlled coordinated reset of neural subpopulations, *Biological Cybernetics* 89 (2003) 81–88.
- [17] P. Goel, B. Ermentrout, Synchrony, stability, and firing patterns in pulse-coupled oscillators, *Physica D: Nonlinear Phenomena* 163 (2002) 191 – 216.
- [18] R. Mirollo, S. Strogatz, Synchronization of pulse-coupled biological oscillators, *SIAM J. Appl. Math.* 50 (1990) 1645–1662.
- [19] S. Bottani, Synchronization of integrate and fire oscillators with global coupling, *Phys. Rev. E* 54 (1996) 2334–2350.
- [20] M. D. LaMar, G. D. Smith, Effect of node-degree correlation on synchronization of identical pulse-coupled oscillators, *Phys. Rev. E* 81 (2010) 046206.
- [21] P. C. Bressloff, S. Coombes, B. de Souza, Dynamics of a ring of pulse-coupled oscillators: Group-theoretic approach, *Phys. Rev. Lett.* 79 (1997) 2791–2794.
- [22] E. Brown, J. Moehlis, P. Holmes, On the phase reduction and response dynamics of neural oscillator populations, *Neural Computation* 16 (2004) 673–715.
- [23] A. Winfree, The geometry of biological time, Springer, 2001.
- [24] B. Ermentrout, Type i membranes, phase resetting curves, and synchrony, *Neural Computation* 8 (1996) 979–1001.
- [25] F. Hoppensteadt, E. Izhikevich, Weakly Connected Neural Networks, Springer-Verlag, New York, 1997.
- [26] V. Novicenko, K. Pyragas, Computation of phase response curves via a direct method adapted to infinitesimal perturbations, *Nonlinear Dynamics* (2011) 1–10. 10.1007/s11071-011-0001-y.
- [27] S. Achuthan, C. Canavier, Phase-resetting curves determine synchronization, phase locking, and clustering in networks of neural oscillators, *The Journal of Neuroscience* 29(16) (2009) 5218–5233.
- [28] E. M. Izhikevich, Dynamical Systems in Neuroscience: The Geometry of Excitability and Bursting, The MIT Press, 2005.

- [29] Y. Kuramoto, Chemical Oscillations, Waves, and Turbulence, Springer, Berlin, 1984.
- [30] S. H. Strogatz, R. E. Mirollo, P. C. Matthews, Coupled nonlinear oscillators below the synchronization threshold: Relaxation by generalized Landau damping 68 (1992) 2730–2733.
- [31] R.-M. Memmesheimer, M. Timme, Designing complex networks, Physica D: Nonlinear Phenomena 224 (2006) 182 – 201. Dynamics on Complex Networks and Applications.
- [32] D.Hansel, G.Mato, C. Meunier, Clustering and slow switching in globally coupled phase oscillators, Phys. Rev. E 48 (1993) 3470–3477.
- [33] L. Lücken, S. Yanchuk, Nonlinear Laser Dynamics – From Quantum Dots to Cryptography, Wiley and Blackwell.
- [34] W. Eckhaus, Studies in Non-Linear Stability Theory, volume 6 of *Springer Tracts in Natural Philosophy*, Springer, New York, 1965.
- [35] M. Wolfrum, S. Yanchuk, Eckhaus instability in systems with large delay, Phys. Rev. Lett 96 (2006) 220201–1–220201–4.